PCCP

Accepted Manuscript




ROYAL SOCIETY OF CHEMISTRY

www.rsc.org/pccp

# Conformational Composition, Molecular Structure and Decomposition of Difluorophosphoryl Azide in the Gas Phase

Zhuang Wu,[a] Hongmin Li,[a] Bifeng Zhu,[a] Xiaoqing Zeng,[a*] Stuart A. Hayes,[b] Norbert W. Mitzel,[b*] Helmut Beckers,[c] and Raphael J. F. Berger[d*]

[a] College of Chemistry, Chemical Engineering and Materials Science, Soochow University, 215123 Suzhou, China. E-mail: xqzeng@suda.edu.cn

[b] Lehrstuhl für Anorganische Chemie und Strukturchemie, Centre for Molecular Materials $CM_2$, Universitätsstraße 15, D-33615 Bielefeld, Germany.

[c] Institut für Chemie und Biochemie, Freie Universität Berlin, 14195 Berlin, Germany.

[d] Materialchemie, Paris-Lodron-Universität Salzburg, Hellbrunner Str. 34, A-5020 Salzburg, Austria. E-mail: Raphael.Berger@sbg.ac.at

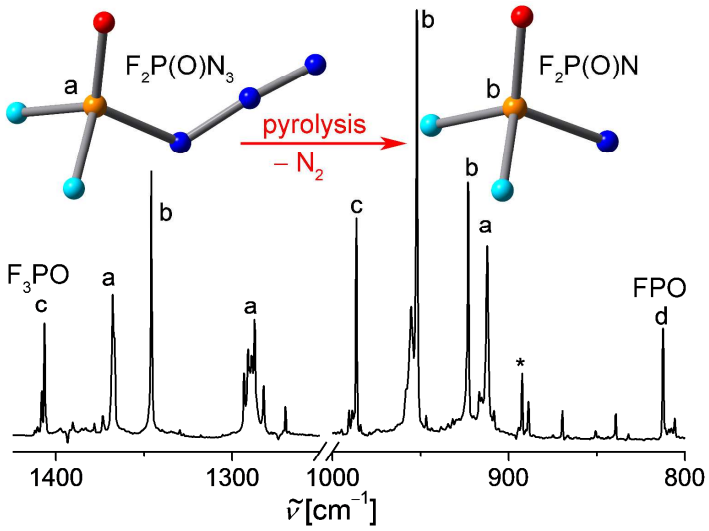


**Abstract:**

The conformational composition, molecular structure and decomposition of difluorophosphoryl azide $F_2P(O)N_3$, in the gas phase was studied by gas electron diffraction (GED), matrix isolation IR spectroscopy, and quantum-chemical calculations respectively. While computational methods predict only minor differences in the total energy between the two possible conformers (*syn* and *anti*), the analysis of electron diffraction data reveals the dominating abundance of the *syn* conformer in the gas phase at room temperature. Ab-initio frequency analyses suggest that a low-frequency large-amplitude motion of the $N_3$ group with respect to the P–N–N–N torsion is to be expected for the *syn* conformer. The large amplitude motion was included explicitly into the GED structure refinement procedure. It presumably contributes to a thermodynamic stabilization of the *syn*-conformer with respect to the *anti*-conformer in the gas phase at ambient temperature. Upon flash vacuum pyrolysis, this *syn* conformer undergoes a stepwise decomposition via the difluorophosphoryl nitrene, $F_2P(O)N$, which features to be the first experimentally observed phosphoryl nitrene that can be thermally produced in the gas phase. To reveal the reaction mechanism, quantum-chemical calculations on the potential energy surface (PES) of $F_2P(O)N_3$ were performed. Both, the B3LYP/6-311+G(3df) and CBS-QB3 calculation results, strongly support a stepwise decomposition into singlet $F_2P(O)N$, which prefers intersystem crossing to the thermally persistent triplet ground state instead of a Curtius rearrangement into FP(O)NF.

**Introduction**

Covalent azides are broadly used in chemistry, biology, and materials science. Their synthesis, structure, and applications have been frequently reviewed in the past few decades.[1–9] Despite the comparatively straightforward preparative access to most covalent azides, their structural characterization has been found to be challenging due to their potentially explosive nature especially in a neat form and with high azide proportion. Thus, it has taken enormous efforts in quite some cases to obtain the structures of small but highly explosive covalent azides like $HN_3$[10] and $XN_3$ (X = F,[11] Cl,[12] Br,[13–14] and I[13,15–16]). As for the metastable parent covalent azides, their characterization is further hampered by facile decomposition at room temperature. For instance, the simplest carbonyl azide $HC(O)N_3$ quickly liberates $N_2$ even at 0 °C in solution, and it forms HNCO through the well-known Curtius rearrangement.[17–18] However, by applying low-temperatures techniques, it has recently been isolated and structurally characterized.[18] Two conformers, *syn* and *anti*, depending on the relative positions of CO and $N_3$ groups with respect to the C–N bond have been spectroscopically identified.

In addition to the fundamental conformational and structural properties, the decomposition of covalent azides has also been the topic of extensive theoretical and experimental studies.[2,19] As for the most frequently investigated carbonyl azides $RC(O)N_3$,[19–25] two decomposition pathways, best known as Curtius rearrangement, have been proposed. One is the stepwise route that occurs by forming a nitrene intermediate RC(O)N upon $N_2$ elimination, as followed by an intramolecular rearrangement to RNCO. The other route happens by $N_2$ elimination with a concerted migration of the R group. According to the calculations, the *syn* conformer prefers a concerted decomposition, whereas the *anti* conformer favors a stepwise mechanism. It should be noted that the activation barrier for the conversion of the two conformers is relatively much lower than the barrier for the $N_2$ elimination of the azide, and the overall decomposition pathway strongly depends on the electronic properties of the substituents.

Very recently, both photolysis and thermolysis of the fluorine-substituted carbonyl azide $FC(O)N_3$[26–27] have been studied. The strong electron inductivity of the fluorine atom enables a stepwise decomposition of this azide, providing a thermally persistent carbonyl nitrene FC(O)N that can be produced in the gas phase.[27] Similar results have also been found for the closely related sulfonyl azide $FS(O)_2N_3$.[28] More excitingly, radicals FCO and $FSO_2$ were obtained as byproducts, which were explained in terms of nitrene dimerization in their triplet ground state as followed by decomposition under the flash vacuum pyrolysis conditions of

$FC(O)N_3$ (Scheme 1a)[27] and $FS(O)_2N_3$ (Scheme 1b),[28] respectively. However, unknown remains the thermal decomposition of the structurally related phosphoryl azide $F_2P(O)N_3$,[29] through which the theoretically predicted radical species $F_2PO$[30] might be generated (Scheme 1c) to complete the link between FPO[31–32] and $F_3PO$.[33]

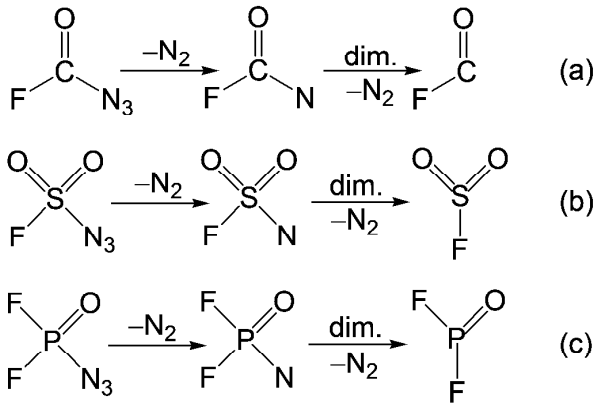


**Scheme 1.** Possible decomposition reactions of $FC(O)N_3$,[27] $FS(O)_2N_3$,[28] and $F_2P(O)N_3$.

In contrast to the carbonyl and sulfonyl counterparts, only very few structurally related phosphoryl azides have been fully characterized.[29,34] Phosphoryl azide $R_2P(O)N_3$ has been considered to be a potentially useful photoaffinity label in biochemistry, and the photochemistry of diaryl- and dialkylphosphoryl azides in solution has been well investigated.[35–41] In all cases, complex photolysis products including derivatives of phosphoryl nitrenes in both singlet and triplet states were obtained.

Up to now, no experimental study on the thermal decomposition of phosphoryl azides has been reported. Despite that the potential energy surfaces (PESs) for the decomposition reactions of $R_2P(O)N_3$ (R = $CH_3$, $CH_3O$) have already been computationally explored in detail.[36] Herein, we report a joint theoretical and experimental study on the molecular structure and thermal decomposition of the simplest phosphoryl azide $F_2P(O)N_3$ in the gas phase. Prior to this study, the structure of this azide in the solid state has been reported,[29] its photo-induced decomposition into $F_2P(O)N$ was observed in solid noble gas matrices, and this triplet nitrene has been unambiguously characterized by IR, EPR, and UV-Vis spectroscopy.[42] We have also reported on the gas-phase structure and the conformational properties of its reduced form the aziodo(difluoro)phosphane $F_2PN_3$.[43] Experimental gas-phase structure determinations of azides are moreover of special interest since these structures may serve as challenging benchmarks for standard single-reference quantum-chemical methods like DFT, HF or MP2. This is already suggested by the various

different possible mesomeric descriptions (electronic resonance) of the $N_3$ group, hinting at possible degenerate forms of differently hybridized molecular orbital configurations. For this reason we have put in addition to our decomposition studies put special emphasis on the experimental determination of the gas-phase structure by electron diffraction.

## Experimental methods

### Sample preparation

Difluorophosphoryl azide, $F_2P(O)N_3$, was synthesized by the reaction of $F_2P(O)Cl$ with $NaN_3$ according to literature.[29] The $^{15}N$-labeled sample was synthesized by using the 1-$^{15}N$ sodium azide (98 atom % $^{15}N$, EURISO-TOP GmbH). The purity of the samples was assured by gas-phase IR spectroscopy.

### Gas electron diffraction

Electron diffraction patterns were recorded using the modified KD-G2 gas diffractometer at Bielefeld University,[44–45] at two camera (nozzle-to-plate) distances (25 and 50 cm) with an accelerating voltage about 60 kV. The sample used for the GED study was purified by trap-to-trap condensation prior to the experiment and was kept at about –10°C during the GED experiment while inlet system and nozzle were held at room temperature. The main conditions of the GED experiment are collected in the Table 1.

**Table 1.** Conditions of the GED experiment.

| Nozzle-to-plate distance, mm | 500.00 | 250.0 | 250.00 |
|---|---|---|---|
| Electron beam current, nA | 150 | 150 | 150 |
| Electron wavelength, Å | 0.04830(1) | 0.04839(1) | 0.04839(1) |
| Exposure time, s | 20–37 | 60-75 | 60–75 |
| Residual gas pressure[a], mbar | $2 \cdot 10^{-5}$ | $3 \cdot 10^{-6}$ | $3 \cdot 10^{-6}$ |

[a]during recording

The wavelength of electrons was determined from diffraction patterns of benzene standard measurements under the same conditions. The molecular intensities $I_{mol}(s)$ were obtained in the $s$-range of 1.6 – 35.6 Å$^{-1}$ [$s = (4\pi/\lambda) \sin\theta/2$, $\lambda$ is electron wavelength and $\theta$ is the scattering angle]. The experimental [and difference = (experimental – theoretical)] intensities $s^4 I_{mol}(s)$ are given in Figure 1. The final $R$-factors of the least-squares refinement were: $R_G$ = 6.34 % and $R_D$ = 4.93%. Details of apparatus, data reduction procedure, employed

structure refinement programs and strategies are described in detail in reference.[44–45]

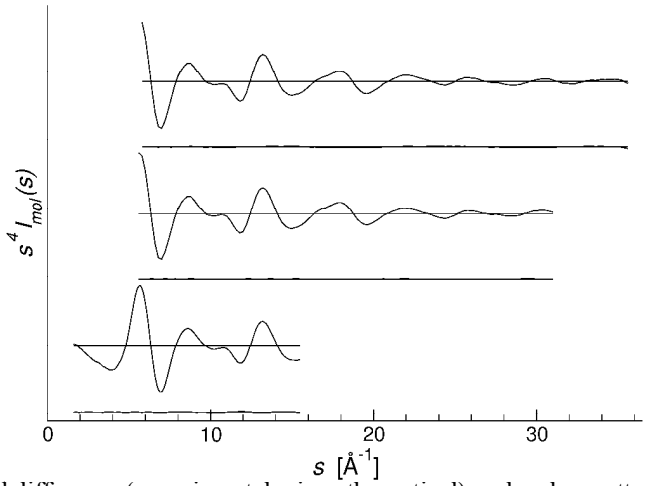


**Fig. 1** Experimental and difference (experimental minus theoretical) molecular scattering intensity curves for $F_2P(O)N_3$.

**Matrix IR spectroscopy**

Matrix IR spectra (4000–500 cm$^{-1}$) were recorded on an FT-IR spectrometer in reflectance mode using a KBr beam splitter and an MCT detector at a resolution of 0.5 cm$^{-1}$. A $F_2P(O)N_3$ sample diluted in argon (1:500) was passed through an aluminum oxide furnace (i.d. 1.0 mm, length 25 mm), which was heated (voltage 6.5 V, current 2.3 A) over a length of ca. 10 mm by tantalum wire (o.d. 0.25 mm, resistance 1.0 Ω). The pyrolysis products were directly deposited onto a cold rhodium-plated copper matrix support at 16 K in high vacuum. While not directly measured, under these conditions, the estimated residence time in the hot zone is well under 1 ms. Details of the matrix apparatus have been described elsewhere.[46] Photolysis experiments were performed using a high-pressure mercury lamp (150 W) by conducting the light through water-cooled quartz lens and an interference (λ=255 nm) filter.

**Calculation details**

The part of the calculations used in the GED analysis were performed using the TURBOMOLE[47] (version 5.9) programme package with def2-TZVPP[48] basis sets for both the HF[49] and MP2[50] levels of theory throughout the study. The MP2 calculations were performed using the RI-MP2[51] routine as it is implemented in TURBOMOLEs ricc2[52] module together with the corresponding auxiliary basis sets.[53]

The remaining quantum chemical calculations were performed using the Gaussian 03 software package.[54]

Ab initio (HF[48] and MP2[49]) and DFT (B3LYP[55]) methods were used at the 6-311+G(3df) basis set. The complete basis set method (CBS-QB3)[56] was also used for accurate energy calculations. The transition states were assured by additional intrinsic reaction coordinate (IRC) calculations.[57–58]

**Calculated potential energy surface of $F_2P(O)N_3$**

Similar to the structurally related carbonyl azides,[19–27] phosphoryl azide $R_2P(O)N_3$, in principle, can adopt a *syn* or an *anti* conformation, depending on the relative position of the PO and $N_3$ groups with respect to the P–N bond (Figure 2). According to the MP2, B3LYP, CBS-QB3 calculations, both conformers are $C_s$ symmetric, and the *syn* conformer of $F_2P(O)N_3$ is predicted slightly lower in energy by 5, 5, and 6 kJ mol$^{-1}$, respectively. This energy difference is close to that predicted for $FC(O)N_3$ (B3LYP/6-311+G(3df): 6 kJ mol$^{-1}$, CBS-QB3: 8 kJ mol$^{-1}$),[27] for which gas electron diffraction (GED) has confirmed the mixture to consist of *syn* (90%) and *anti* (10%) conformers at room temperature.[59] As for $F_2P(O)N_3$, the activation barrier for the conversion of the *syn* into the *anti* conformer is merely 10 kJ mol$^{-1}$ (CBS-QB3), which is significantly lower than that of $FC(O)N_3$ (39 kJ mol$^{-1}$)[27] at the same theoretical level. The structure of the corresponding transition state (TS1, Figure 3) exhibits an F-P-N-N dihedral angle of –15.6°, and the vibrational displacement vector of the imaginary frequency (59*i* cm$^{-1}$) suggests a rotation of the $N_3$ group around the bridging P–N bond.

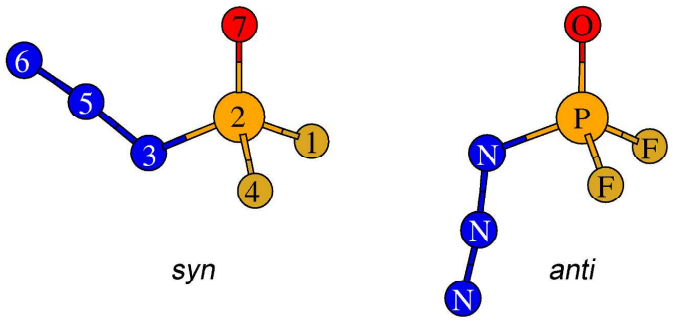


**Fig. 2** *Syn* and *anti* conformers of $F_2P(O)N_3$ with atomic numbering for the GED structure refinement of the *syn* conformer.

To probe the thermal stabilities of these two conformers, the transition states, TS2 (*syn*) and TS3 (*anti*), leading to the $N_2$ elimination were computationally located. The B3LYP predicted activation barriers, 250

and 204 kJ mol$^{-1}$, are much higher than those of *syn* (170 kJ mol$^{-1}$) and *anti* (140 kJ mol$^{-1}$) $FC(O)N_3$[27] at the same theoretical level. The higher thermal stability of phosphoryl azides compared to that of carbonyl azides can also be inferred by the CBS-QB3 calculated decomposition barriers of $(CH_3)_2P(O)N_3$ (189 kJ mol$^{-1}$) and $(CH_3O)_2P(O)N_3$ (175 kJ mol$^{-1}$)[36] than $CH_3C(O)N_3$ (113 kJ mol$^{-1}$) and $CH_3OC(O)N_3$ (126 kJ mol$^{-1}$).[60] The attempts to locate TS3 by using the CBS-QB3 method failed, however, the reliability of the B3LYP optimized geometries of TS2 and TS3 were approved by using the MP2 method at the same 6-311+G(3df) basis set, and also TS2 is higher by 56 kJ mol$^{-1}$.

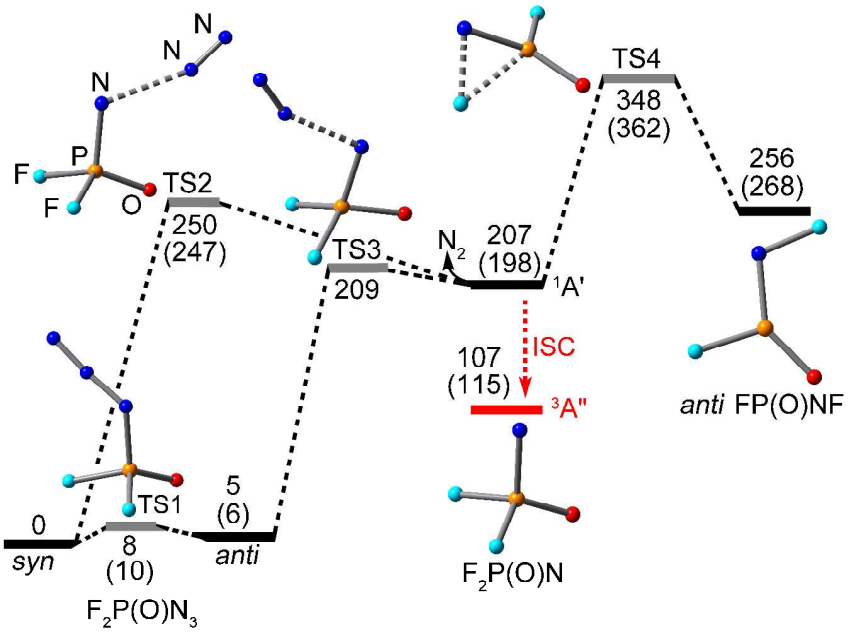


**Fig. 3** Calculated relative energies (kJ mol$^{-1}$) of the minima and transition states for the decomposition of $F_2P(O)N_3$ at the B3LYP/6-311+G(3df) level of theory. The relative energies calculated at the CBS-QB3 level are given in parenthesis. The intersystem crossing (ISC) from the singlet ($^1$A') to the triplet ($^3$A") state of $F_2P(O)N$ is shown with an arrowhead.

According to the early calculation study,[36] two distinct transition states for both concerted and stepwise decomposition pathways of organic phosphoryl azides $(CH_3)_2P(O)N_3$ and $(CH_3O)_2P(O)N_3$ were found and confirmed by intrinsic reaction coordinate (IRC) analysis, although no conformational information of the azides was given. As for $(CH_3)_2P(O)N_3$, fairly close activation barriers of 190 (concerted to $CH_3P(O)NCH_3$ + $N_2$) and 189 kJ mol$^{-1}$ (stepwise to $(CH_3)_2P(O)N$ + $N_2$) were predicted at the CBS-QB3 level.[36] In contrast, for the methoxy analogue, the stepwise decomposition to the nitrene $(CH_3O)_2P(O)N$ (175 kJ mol$^{-1}$) is clearly

lower in energy than the concerted to the rearrangement product $CH_3OP(O)NOCH_3$ (197 kJ $mol^{-1}$).[36] Surprisingly, the IRC analysis of TS2 and TS3 for $F_2P(O)N_3$ demonstrates that both lead to the formation of the singlet nitrene $F_2P(O)N$ (Figure 3), all the attempts to locate the transition state for the concerted pathway failed. Therefore, it can be concluded that thermolysis of $F_2P(O)N_3$ would exclusively furnish nitrene $F_2P(O)N$ as the initial intermediate. Interestingly, singlet phosphoryl nitrene $F_2P(O)N$ seems to be highly reactive towards $N_2$ as indicated by the rather close energy of $F_2P(O)N + N_2$ to TS3 (Figure 3). This calculation result coincides with the previous experimental observation that $F_2P(O)N_3$ was formed by UV irradiation (255 nm) from $F_2P(O)N$ in the presence of $N_2$ in solid argon matrix at 16 K.[42]

As a key factor for the thermal stability of transient α-oxo nitrene species, the activation barrier for the fluorine-shifted Curtius type rearrangement was also considered for singlet $F_2P(O)N$. In agreement with the previous B3LYP calculation, the best CBS-QB3 method predicts a large barrier of 164 kJ $mol^{-1}$, which is even greater than that required for the decomposition of the room-temperature stable azide $FC(O)N_3$ (132 kJ $mol^{-1}$, CBS-QB3).[27] Thus, singlet $F_2P(O)N$ would be a candidate species for observation if there were no competing processes. However, both B3LYP and CBS-QB3 calculations show that this nitrene has a triplet ground state, and the energy gap to the singlet ($\Delta E_{ST}$) is as large as 83 kJ $mol^{-1}$ at the CBS-QB3 level. This is larger than other theoretically studied phosphoryl nitrenes such as $(CH_3)_2P(O)N$ (66 kJ $mol^{-1}$) and $(CH_3O)_2P(O)N$ (58 kJ $mol^{-1}$)[36] and also the other two fluorinated α-oxo nitrenes $FS(O)_2N$ (57 kJ $mol^{-1}$)[28] and FC(O)N (33 kJ $mol^{-1}$)[27] at the same theoretical level. It should be noted that both $FS(O)_2N$ and FC(O)N in their triplet ground state have been thermally produced in the gas phase by flash vacuum pyrolysis of the respective azide precursors.[27–28] Therefore, the initially generated singlet $F_2P(O)N$ may also relax to the lower-energy triplet ground through intersystem crossing (ISC) before its rearrangement. More importantly, the thermal persistency of the triplet can be partially inferred by inefficient reverse ISC due to large $\Delta E_{ST}$, and also the supposed rearrangement triplet FP(O)NF, not calculated, but is expected to be exceedingly higher than that of the triplet nitrene. Therefore, the overall PES of $F_2P(O)N_3$ strongly suggest that triplet nitrene $F_2P(O)N$ should be accessible in the gas phase upon thermolysis of $F_2P(O)N_3$.

**Calculated structures of $F_2P(O)N$ dimer and related species**

Considering the formation and subsequent decomposition of triplet $F_2P(O)N$ dimer $F_2P(O)NNP(O)F_2$ in the gas phase, its molecular structures and possible decomposition intermediates (Figure 4) were fully optimized

at the B3LYP/6-311+G(3df) level.

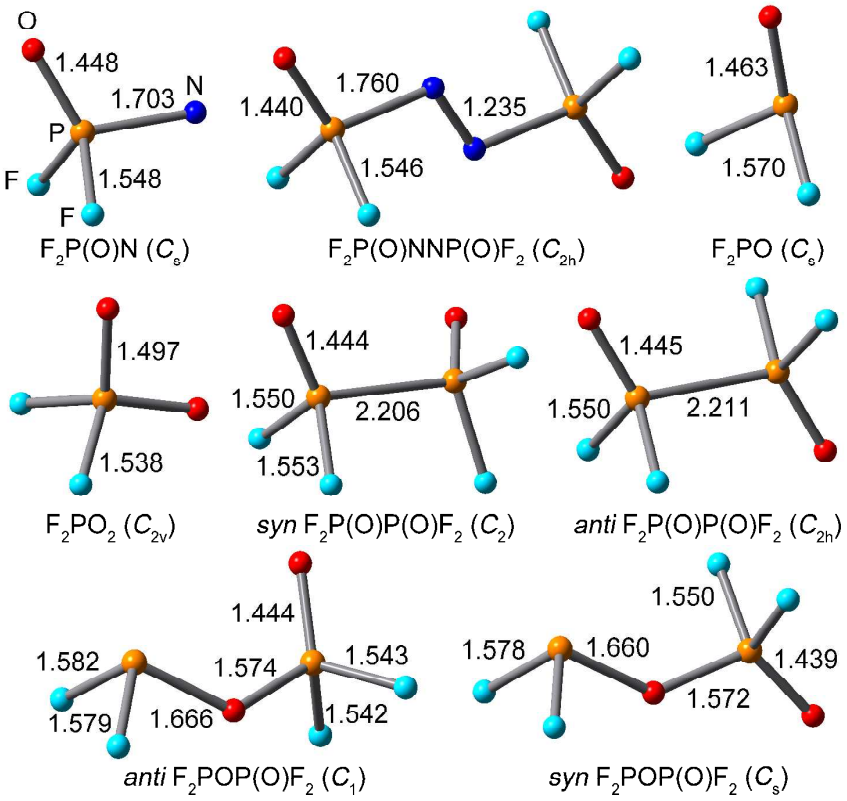


**Fig. 4** Calculated molecular structures of $F_2P(O)NNP(O)F_2$ and related species at the B3LYP/6-311+G(3df) level. Bond lengths (Å) and molecular symmetries (in parentheses) are shown.

Similar to the well-known azobenzene,[61] the minimum structure of the nitrene dimer $F_2P(O)NNP(O)F_2$ exhibits a planar *anti* conformation of the P–N=N–P backbone. The calculated central N=N bond in $F_2P(O)NNP(O)F_2$ (1.235 Å) is even shorter than that calculated for *anti* azobenzene (1.268 Å MP2/cc-pVTZ; 1.247 Å single crystal X-ray diffraction),[62] whereas, the P–N bond (1.760 Å) is longer than that in the triplet nitrene $F_2P(O)N$ (1.703 Å). These structural features indicate that this dimer is probably thermally instable towards to the dissociation into $N_2$ + 2 $F_2PO$. The most likely decomposition product, the radical $F_2PO$, is experimentally unknown. Only its structure and bond dissociation energies have been calculated at the CCSD(T)/aug-cc-pV(Q+d)Z level.[30] The structural parameters calculated at the B3LYP/6-311+G(3df) level (P–F 1.570 Å, P–O 1.463 Å, F–P–F 98.9°, F–P–O 115.4°) nicely reproduce the results obtained using the highly demanding calculation method (P–F 1.558 Å, P–O 1.465 Å, F–P–F 98.9°, F–P–O 115.9°). The elusive oxyl radical $F_2PO_2$,[62] as the potential oxidation product of $F_2PO$, was also structurally optimized (Figure 4).

This $C_{2v}$ symmetric molecule has one electron more than the nitrene $F_2P(O)N$. Its existence was first claimed based on a UV spectrum which was eventually confirmed to belong to OClO.[42]

Additionally, molecules with a composition of $F_4P_2O_2$, including a P–P bonded $F_2P(O)–P(O)F_2$ and P–O bonded $F_2PO–P(O)F_2$ might be formed from either decomposition of $F_2P(O)NNP(O)F_2$ or dimerization of two $F_2PO$ radicals. The optimized structures of these two isomers are shown in Figure 4, and both have close-in-energy *syn* and *anti* conformers. Interestingly, $F_2PO–P(O)F_2$ is more stable than $F_2P(O)–P(O)F_2$ by 84 and 80 kJ mol$^{-1}$ at the B3LYP/6-311+G(3df) and CBS-QB3 levels, respectively. This reasonably explains the early experimental observations that $F_2PO–P(O)F_2$ and not $F_2P(O)–P(O)F_2$ was obtained as the photolysis (254 nm) product of $F_2P(O)Br$ in the presence of mercury at 23 °C.[63] Despite the molecular structure of $F_2PO–P(O)F_2$ has not been determined, its unsymmetrical structure has been unambiguously proven by IR and NMR spectroscopy.[63–64] It was also noticed that this compound decomposes completely after 18 hours at room temperature in a sealed glass tube.[64]

**Gas-phase structure of $F_2P(O)N_3$**

As also outlined above, for $F_2P(O)N_3$, two possible conformations may exist, in which the $N_3$ group adopt either the *syn* or the *anti* position with respect to the P=O moiety, as shown in Figure 2. At both HF/TZVPP and MP2/TZVPP level of theory the *syn* conformer is slightly lower in energy (11 and 7 kJ mol$^{-1}$) than the *anti* conformer. For this reason we have attempted fitting a two conformer model to the experimental data, which resulted in minimal *R*-factors for 0% contribution of the *anti*-conformer. Hence the final structure model used for refinement contains solely the *syn* conformer.

Calculated structure parameters for two conformers of $F_2P(O)N_3$ of $C_s$ symmetry are listed in Table 1. Remarkably the difference between HF and MP2 values of the formally (partial) triple bonded N5-N6 atoms from the azido group is significant. This is a hint for a possible non-negligible admixture of other configuration state functions to the ground-state wave function. Hence similar considerations were made for the case of $F_2PN_3$.[43]

Calculations predict a large-amplitude torsional mode for the $N_3$ moiety (35 cm$^{-1}$ at the MP2/TZVPP level of theory). In order to simulate the dynamic behavior of the azide unit in the electron diffraction experiment, nine pseudo conformers with different F-P-N-N torsion angles were included into the refinement. The validity of this strategy could be verified by yielding implausible ∠(N3-N5-N6) angles around 180 to 185°

when refining a rigid one-conformer structure model.

Ten degrees of freedom for the description of the molecular geometry have to be accounted for in the structure model of *syn*-$F_2P(O)N_3$ in $C_s$ symmetry. These parameters are listed in Table 2. In addition one more parameter was use to describe to torsional dynamics of the azido moiety. The torsion dynamics of the azide group relative to the O=P moiety was described using [$\tau$(O–P–N3–N5)] nine equally weighted pseudo-conformers $anti_i$ ($i$ = 1,..,9) with different angles $\tau = \tau_{max}\ i^2/81$ ranging from 0° to a maximum angle $\tau_{max}$ and by using increasing incremental angle differences. In this way a monotonically decreasing population density of $\tau$ is modeled without introducing further assumptions about the underlying potential or state population. $\tau_{max}$ was refined as an independent parameter [yielding a value of 28(3)°]. In this way a total of 11 parameters for the least-squares refinement resulted.

All ten structure parameters could be refined independently and without restraints, resulting in only two parameter pairs correlated stronger than 68%: $r$(P–F),$r$(P–N) = 83% and ∠(F–P–F), ∠(F–P–F) = 88%.

**Table 2.** Calculated and experimentally determined gas-phase structure parameters of *syn* $F_2P(O)N_3$.

| parameters[a] | HF[b] | MP2[b] | B3LYP[b] | XRD[c] | GED[d] |
|---|---|---|---|---|---|
| $r$(N6–N5) | 1.077 | 1.144 | 1.118 | 1.115(3) | 1.130(2) |
| $r$(N3–N5) | 1.241 | 1.236 | 1.235 | 1.251(3) | 1.251(3) |
| $r$(P–F) | 1.509 | 1.540 | 1.546 | 1.525(2) | 1.5316(6) |
| $r$(P–N) | 1.636 | 1.660 | 1.663 | 1.639(2) | 1.657(2) |
| $r$(P=O) | 1.421 | 1.449 | 1.446 | 1.445(2) | 1.437(4) |
| ∠(F–P–F) | 99.1 | 99.0 | 99.0 | 98.8(2) | 98.8(3) |
| ∠(O–P–N3) | 117.6 | 118.1 | 118.7 | 120.1(2) | 118.9(3) |
| ∠(F–P–N3) | 103.0 | 101.6 | 101.7 | 102.7(2) | 101.1(7) |
| ∠(P–N3–N5) | 117.0 | 118.4 | 120.2 | 117.9(2) | 117.8(5) |
| ∠(N3–N5–N6) | 174.8 | 173.4 | 173.7 | 172.9(3) | 172(2) |

[a] Bond lengths [Å] and angles [°]. [b] def2-TZVPP basis set. [c]Averaged structure of two crystallographically non-equivalent molecules in the unit cell, see reference [29]. [d]Gas phase $r_{h1}$ structure type, errors are given as 1 σ

The interatomic amplitudes of vibration were partitioned into eleven groups according to the distances of the atoms pairs involved. The relative ratio of the amplitudes of each of these groups were kept constant at the values calculated by the program SHRINK[65] based on a harmonic force field analysis at the MP2/TZVPP level of theory. In this calculation of the amplitudes of vibration the $\tau$ mode was excluded from the Hessian since this mode is modeled using the pseudo-conformers. The eleven independent amplitudes were refined unrestrained. It should be noted that part of the determined parameter differences are strongly correlated to

interatomic vibrational amplitudes. A complete listing of independently refined, calculated and dependent amplitudes is given in Table S1 (ESI‡).

The radial distribution curve is given in Figure 5. Final *R*-factors from the refinement are $R_D$ = 4.93 % and $R_G$ = 6.34 %. In general there is a very good agreement between GED structure parameters and the respective computational values. All experimental structural parameters are in size between the HF and the MP2 values (slightly closer to the MP2), which both are in good agreement with the only one significant exception being the distance between atoms N3 and N5. And although quantum-chemical calculations, as outlined above, suggest only minor differences in total electronic energies between the two possible conformers *syn* and *anti*, the gas-phase diffraction data were consistent already within a one conformer model (*syn*) and yielded worse fits when arbitrary amounts of *anti* conformer were added. An explanation for this observation might be found in the presence of the very low-frequent torsional mode of vibration of the $N_3$ moiety in the *syn* conformer (35 $cm^{-1}$ at MP2/TZVPP level of theory) where as the analogous torsional mode in the *anti* conformer is calculated to 58 $cm^{-1}$. The difference in the vibrational energy levels between the two conformers propagate into a calculated free energy difference of 1 kJ $mol^{-1}$ at 298.15 K (in favor of the *syn*-conformer), where the largest contribution to these originating from the strongest occupied lowest modes. When considering such a small calculated free energy difference $\Delta G^{297}$ of about 7 kJ $mol^{-1}$ (6.6 kJ $mol^{-1}$ electronic energy difference (MP2) and 1.1 kJ $mol^{-1}$ chemical potential difference) between the *syn* and *anti* conformer, it must be recalled that the calculated frequencies based on (a) the harmonic approximation and (b) numerical gradients will be especially prone to error. Accuracies of a few kJ $mol^{-1}$ in electronic energy might be achieved for single reference standard cases with highly correlated methods of computation at most but will be hardly be achieved for dynamic properties in molecules with low lying presumably anharmonic modes of vibration. Due to the possible partial multi-reference character of the electronic ground states of azide moiety containing molecules, the experimental evidence for the dominant abundance of the *syn* conformer in the gas phase at ambient conditions is of high importance.

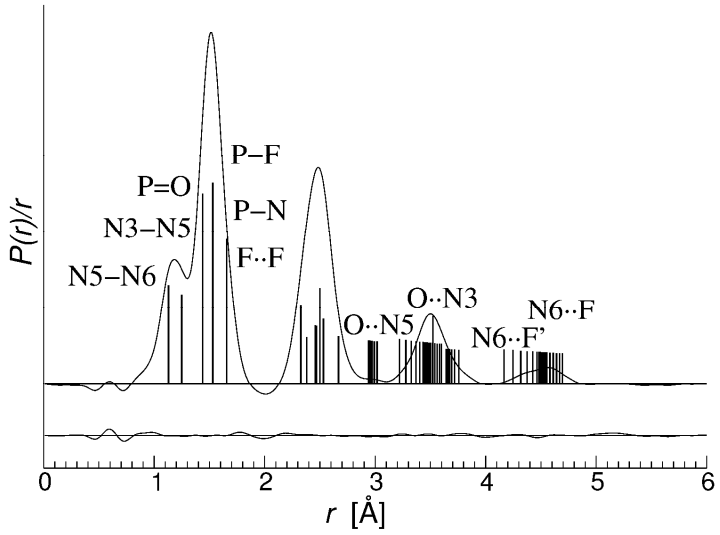


**Fig. 5** Radial distribution curve, difference (experimental minus theoretical) curve and model from the GED structure refinement of $F_2P(O)N_3$. The multitude of theoretical distance bars in the region above 3 Å reflects the dynamic pseudo conformer model.

**Flash vacuum pyrolysis of $F_2P(O)N_3$**

Thermolysis of $F_2P(O)N_3$ in an argon dilution (1:500) at ca. 800 °C was carried out. The resulting IR spectrum of the matrix-isolated decomposition products is shown in Figure 6B. Comparing to the IR spectrum of the precursor (Figure 6A), only small amount of the azide was left upon pyrolysis. Among the decomposition products, the formation of FPO ($\nu$(PO) = 1293, $\nu$(PF) = 812 $cm^{-1}$)[31] and $F_3PO$ ($\nu$(PO) = 1406, $\nu(PF_3)_{antisym}$ = 986, $\nu(PF_3)_{sym}$ = 869 $cm^{-1}$)[66] can be assured by referring to their known IR data. The presence of the triplet nitrene species $F_2P(O)N$ ($\nu$(PO) = 1346, $\nu(PF_2)_{antisym}$ = 952, $\nu(PF_2)_{sym}$ = 923, $\nu$(PO) = 764 $cm^{-1}$)[42] can be further ascertained by both the $^{15}N$-isotopic shifts of these bands and its known sensitivity to the UV irradiation of 255 nm, under which it efficiently converts into $F_2PNO$ (Figure 6C).

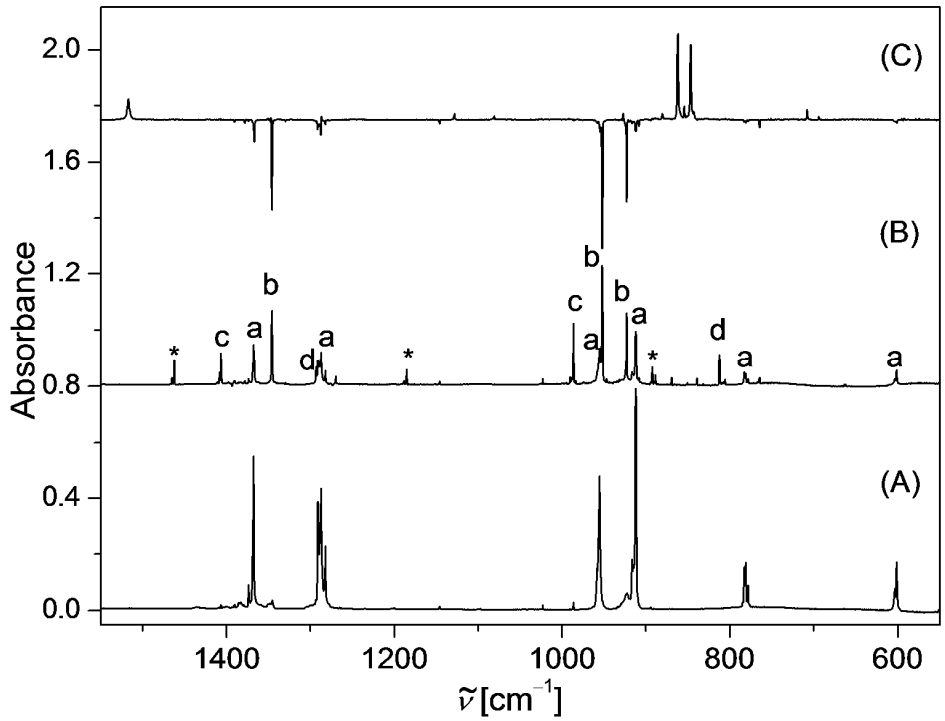


**Fig. 6** (A) IR spectrum (1550–550 cm$^{-1}$) of Ar-matrix isolated $F_2P(O)N_3$, (B) IR spectrum of Ar-matrix isolated pyrolysis products (ca. 800 °C), and (C) IR difference spectrum showing the changes after irradiation ($\lambda$ = 255 nm, 25 min) of the matrix associated with spectrum B. The IR bands of $F_2P(O)N_3$ (a), $F_2P(O)N$ (b), $F_3PO$ (c), FPO (d), and unknown species (*) are labeled in spectrum B. The IR bands of $F_2PNO$ point upwards in spectrum C.

As has been mentioned above, decomposition products FCO and $FSO_2$ of the nitrene dimer in the gas phase for triplet FC(O)N and $FSO_2N$ were also obtained by flash pyrolysis of $FC(O)N_3$[27] and $FSO_2N_3$[28] (Scheme 1), respectively. To search for the novel radical species $F_2PO$, presumably formed by decomposition of the triplet $F_2P(O)N$ dimer, calculations on its IR spectrum were performed. At the B3LYP/6-311+G(3df) level of theory, this $C_s$ symmetric radical was calculated to have IR fundamental vibrations at 1259, 859, 812, 446, 350, and 347 cm$^{-1}$. The first three IR bands have strong IR intensities of 113, 192, and 97 km mol$^{-1}$, implying that they could be identified in the present spectral range of 1550–550 cm$^{-1}$. Indeed, there are a few new weak IR bands at 1462, 1185, 892, 840, and 764 cm$^{-1}$, all of which show no $^{15}$N-isotpic shift when $^{15}$N-enriched $F_2P(O)N_3$ was employed. However, the unexpected discrepancy between the observation and prediction precludes a clear identification of $F_2PO$. Nevertheless, the presence of FPO and $F_3PO$ among the pyrolysis

products of $F_2P(O)N_3$ seems to support bimolecular reaction of $F_2PO$ which leads to its dismutation into FPO and $F_3PO$ under the pyrolysis conditions.

## Conclusion

The molecular structure of $F_2P(O)N_3$ in the gas phase at ambient temperature was determined experimentally by electron diffraction. One conformer with the PO and $N_3$ units being in *syn* position was found. Despite a theoretically possible multi-reference character of the ground-state wave function, all $r_{h1}$ structure parameters were found in the range between the equilibrium structure ($r_e$) values. These HF and MP2 values are generally in good agreement, except the formally triply bonded N5–N6 distance. This distance at 1.130(2) Å in the experiment is closer to the MP2 value of 1.144 Å than to the HF value of 1.077 Å.

Upon flash pyrolysis, the *syn* conformer of $F_2P(O)N_3$ decomposes into a mixture of triplet nitrene $F_2P(O)N$, FPO, $F_3PO$, and other unknown products. The gas phase formation of $F_2P(O)N$ is a rare example of phosphoryl nitrenes that is thermally persistent for further structural and reactivity studies. No expected secondary decomposition product ($F_2PO$) of the nitrene dimer $F_2P(O)NNP(O)F_2$ could be obtained. To account for the experimental observations, quantum-chemical calculations on the potential energy surface for the thermal decomposition of $F_2P(O)N_3$ were performed, and the molecular structures of possible intermediates were also fully optimized by quantum-chemical methods. These theoretical results clearly support a stepwise decomposition of $F_2P(O)N_3$ via the nitrene intermediate $F_2P(O)N$. For this initially generated singlet nitrene, the high Curtius rearrangement barrier (164 kJ $mol^{-1}$, CBS-QB3) and large energy separation to the triplet ground state (83 kJ $mol^{-1}$) facility the electronic relaxation to the thermally persistent triplet.

## Acknowledgements

This work was supported by the National Natural Science Foundation of China (21372173, 21422304), and the Beijing National Laboratory for Molecular Sciences (20140128). N. W. M. acknowledges the support from the Deutsche Forschungsgemeinschaft for the Core Facility GED@BI (MI-477/21-1). X. Z. gratefully acknowledges Prof. H. Willner for his generous support during a research stay in Bergische Universität Wuppertal, Germany.

**Electronic Supplementary Information (ESI)** available: Calculated atomic coordinates and energies of all species discussed, gas-phase electron diffraction structure refinement data.

**References**


[1] S. Bräse and K. Banert, *Organic Azides: Syntheses and Applications*, Wiley, Chichester, **2010**.

[2] R. A. Moss, M. S. Platz and M. J. Jones, *Reactive Intermediates*, Wiley-Interscience, **2004**.

[3] E. F. V. Scriven, *Azides and Nitrenes; Reactivity and Utility*, Academic Press Inc., New York, **1984**.

[4] P. Portius and M. Davis, *Coord. Chem. Rev.*, 2013, **257**, 1011.

[5] L. H. Liu and M. D. Yan, *Acc. Chem. Res.*, 2010, **43**, 1434.

[6] S. Bräse, C. Gil, K. Knepper and V. Zimmermann, *Angew. Chem. Int. Ed.*, 2005, **44**, 5188.

[7] C. Knapp and J. Passmore, *Angew. Chem. Int. Ed.*, 2004, **43**, 834.

[8] T. M. Klapötke, *Chem. Ber.*, 1997, **130**, 443.

[9] I. C. Tornieporth-Oetting and T. M. Klapötke, *Angew. Chem. Int. Ed. Engl.*, 1995, **34**, 511.

[10] J. Evers, M. Göel, B. Krumm, F. Martin, S. Medvedyev, G. Oehlinger, F. X. Steemann, I. Troyan, T. M. Klapötke and M. I. Eremets, *J. Am. Chem. Soc.*, 2011, **133**, 12100, and references therein.

[11] D. Christen, H. G. Mack, G. Schatte and H. Willner, *J. Am. Chem. Soc.*, 1988, **110**, 707.

[12] M. Hargittai, I. C. Tornieporth-Oetting, T. M. Klapötke, M. Kolonits and I. Hargittai, *Angew. Chem. Int. Ed.*, 1993, **32,** 759.

[13] B. Lyhs, D. Bläser, C. Wölper, S. Schulz and G. Jansen, *Angew. Chem. Int. Ed.*, 2012, **51**, 12859, and references therein.

[14] B. Lyhs, D. Bläser, C. Wölper, S. Schulz and G. Jansen, *Angew. Chem. Int. Ed.*, 2012, **51**, 1970, and references therein.

[15] P. Buzek, T. M. Klapötke, P. v. R. Schleyer, I. C. Tornieporth-Oetting and P. S. White, *Angew. Chem. Int. Ed.*, 1993, **32**, 275.

[16] M. Hargittai, J. Molnar, T. M. Klapötke, I. C. Tornieporth-Oetting, M. Kolonits and I. Hargittai, *J. Phys. Chem.*, 1994, **98**, 10095.

[17] K. Banert, C. Berndt, M. Hagedorn, H. Liu, T. Anacker, J. Friedrich and G. Rauhut, *Angew. Chem. Int. Ed.*, 2012, **51**, 4718.

[18] X. Q. Zeng, E. Bernhardt, H. Beckers, K. Banert, M. Hagedorn, H. Liu, *Angew. Chem. Int. Ed.*, 2013, **52**, 3503.

[19] D. E. Falvey and A. D. Gudmundsdottir, *Nitrenes and Nitrenium Ions (Wiley Series of Reactive Intermediates in Chemistry and Biology)*, Vol. 6; John Wiley & Sons, Inc., New York, 2013.

[20] J. Kubicki, Y. Zhang, J. Xue, H. L. Luk and M. Platz, *Phys. Chem. Chem. Phys.*, 2012, **14**, 10377.

[21] E. A. Pritchina, N. P. Gritsan, A. Maltsev, T. Bally, T. Autrey, Y. Liu, Y. Wang and J. P. Toscano, *Phys. Chem. Chem. Phys.*, 2003, **5**, 1010.

[22] J. Kubicki, Y. Zhang, S. Vyas, G. Burdzinski, H. L. Luk, J. Wang, J. Xue, H. -L. Peng, E. A. Pritchina, M. Sliwa, G. Buntinx, N. P. Gritsan, C. M. Hadad and M. S. Platz, *J. Am. Chem. Soc.*, 2011, **133**, 9751.

[23] J. Kubicki, Y. Zhang, J. Wang, H. L. Luk, H. -L. Peng, S. Vyas and M. S. Platz, *J. Am. Chem. Soc.*, 2009, **131**, 4212.

[24] C. Wentrup and H. Bornemann, *Eur. J. Org. Chem.*, 2005, **21**, 4521.

[25] J. M. Dyke, G. Levita, A. Morris, J. S. Ogden, A. A. Dias, M. Algarra, J. P. Santos, M. L. Costa, P. Rodrigues, M. M. Andrade and M. T. Barros, *Chem. Eur. J.*, 2005, **11**, 1665.

[26] X. Q. Zeng, H. Beckers, H. Willner, D. Grote and W. Sander, *Chem. Eur. J.*, 2011, **17**, 3977.

[27] H. L. Sun, B. F. Zhu, Z. Wu, X. Q. Zeng, H. Beckers and W. S. Jenks, *J. Org. Chem.*, 2015, **80**, 2006.

[28] X. Q. Zeng, H. Beckers and H. Willner, *J. Am. Chem. Soc.*, 2013, **135**, 2096.

[29] X. Q. Zeng, M. Gerken, H. Beckers and H. Willner, *Inorg. Chem.*, 2010, **49**, 3002.

[30] D. J. Grant, M. H. Matus, J. R. Switzer, D. A. Dixon, J. S. Francisco and K. O. Christe, *J. Phys. Chem. A*, 2008, **112**, 3145.

[31] R. Ahlrichs, R. Becherer, M. Binnewies, H. Borrmann, M. Lakenbrink, S. Schunck and H. Schnöckel, *J. Am. Chem. Soc.*, 1986, **108**, 7905.

[32] H. Beckers, H. Bürger, P. Paplewski, M. Bogey, J. Demaison, P. Dréan, A. Walters, J. Breidung and W. Thiel, *Phys. Chem. Chem. Phys.*, 2001, **3**, 4247.

[33] M. Feller, K. Lux and A. Kornath, *Z. Anorg. Allg. Chem.*, 2014, **640**, 53, and references therein.

[34] X. Q. Zeng, E. Bernhardt, H. Beckers and H. Willner, *Inorg. Chem.*, 2011, **50**, 11235.

[35] S. H. Kim, S. H. Park, J. H. Choi and S. Chang, *Chem. Asian J.*, 2011, **6**, 2618, and references therein.

[36] R. D. McCulla, G. A. Gohar, C. M. Hadad and M. S. Platz, *J. Org. Chem.*, 2007, **72**, 9426.

[37] G. A. Gohar and M. S. Platz, *J. Phys. Chem. A*, 2003, **107**, 3704.

[38] S. Vyas, S. Muthukrishnan, J. Kubicki, R. D. McCulla, G. Burdzinski, M. Sliwa, M. S. Platz and C. M. Hadad, *J. Am. Chem. Soc.*, 2010, **132**, 16796, and references therein.

[39] R. Breslow, A. Feiring and F. Herman, *J. Am. Chem. Soc.*, 1974, **96**, 5937.

[40] P. Maslak, *J. Am. Chem. Soc.*, 1989, **111**, 8201.

[41] M. Houser, S. Kelley, V. Maloney, M. Marlow, K. Steininger, and H. Zhou, *J. Phys. Chem. A*, 1995, **99**, 7946.

[42] X. Q. Zeng, H. Beckers, H. Willner, P. Neuhaus, D. Grote and W. Sander, *Chem. Eur. J.*, 2009, **15**, 13466.

[43] X. Q. Zeng, H. Beckers, H. Willner, R. J. F. Berger, S. A. Hayes, N. W. Mitzel, *Eur. J. Inorg. Chem.,* **6**, 2011, 896.

[44] R. J. F. Berger, M. Hoffmann, S. A. Hayes and N. W. Mitzel, *Z. Naturforsch.*, 2010, **64b**, 1259.

[45] M. Hagemann, R. J. F. Berger, S. A. Hayes, H.-G. Stammler and N. W. Mitzel, *Chem. Eur. J.*, 2008, **14**, 11027.

[46] H. G. Schnöckel and H. Willner, *Infrared and Raman Spectroscopy, Methods and Applications*, VCH: Weinheim, 1994.

[47] a) R. Ahlrichs, M. Bär, M. Häser, H. Horn and C. Kölmel, *Chem. Phys. Lett.* 1989, **162**, 165; b) M. Häser and R. Ahlrichs, *J. Comput. Chem.* 1989, **10**, 104.

[48] F. Weigend, F. Furche and R. Ahlrichs, *J. Chem. Phys.* 2003, **119**, 12753.

[49] C. C. J. Roothaan, *Rev. Mod. Phys.*, 1951, **23**, 69.

[50] C. Møller and M. S. Plesset, *Phys. Rev.*, 1934, **46**, 618.

[51] F. Haase and R. Ahlrichs, *J. Comp. Chem.* 1993, **14**, 907.

[52] C. Hättig, *J. Chem. Phys.* 2003, **118**, 7751.

[53] C. Hättig, C. *Phys. Chem. Chem. Phys.* 2005, **7**, 59.

[54] M. J. Frisch, G. W. Trucks, H. B. Schlegel, G. E. Scuseria, M. A. Robb, J. R. Cheeseman, J. A.

Montgomery, T. Vreven, K. N. Kudin, J. C. Burant, J. M. Millam, S. S. Iyengar, J. Tomasi, V. Barone, B. Mennucci, M. Cossi, G. Scalmani, N. Rega, G. A. Petersson, H. Nakatsuji, M. Hada, M. Ehara, K. Toyota, R. Fukuda, J. Hasegawa, M. Ishida, T. Nakajima, Y. Honda, O. Kitao, H. Nakai, M. Klene, X. Li, J. E. Knox, H. P. Hratchian, J. B. Cross, C. Adamo, J. Jaramillo, R. Gomperts, R. E. Stratmann, O. Yazyev, A. J. Austin, R. Cammi, C. Pomelli, J. W. Ochterski, P. Y. Ayala, K. Morokuma, G. A. Voth, P. Salvador, J. J. Dannenberg, V. G. Zakrzewski, S. Dapprich, A. D. Daniels, M. C. Strain, O. Farkas, D. K. Malick, A. D. Rabuck, K. Raghavachari, J. B. Foresman, J. V. Ortiz, Q. Cui, A. G. Baboul, S. Clifford, J. Cioslowski, B. B. Stefanov, G. Liu, A. Liashenko, P. Piskorz, I. Komaromi, R. L. Martin, D. J. Fox, T. Keith, M. A. Al-Laham, C. Y. Peng, A. Nanayakkara, M. Challacombe, P. M. W. Gill, B. Johnson, W. Chen, M. W. Wong, C. Gonzalez and J. A. Pople, *Gaussian 03, Revision D.01*, Gaussian, Inc., Pittsburgh PA, 2003.

[55] A. D. Becke, *J. Chem. Phys.*, 1993, **98**, 5648.

[56] J. A. Montgomery, M. J. Frisch, J. W. Ochterski and G. A. Petersson, *J. Chem. Phys.*, 2000, **112**, 6532.

[57] C. Gonzalez and H. B. Schlegel, *J. Chem. Phys.*, 1989, **90**, 2154.

[58] C. Gonzalez and H. B. Schlegel, *J. Phys. Chem.*, 1990, **94**, 5523.

[59] H.-G. Mack, C. O. Della Védova and H. Willner, *J. Mol. Struct.*, 1993, **291**, 197.

[60] J. Liu, S. Mandel, C. M. Hadad and M. S. Platz, *J. Org. Chem.*, 2004, **69**, 8583.

[61] H. Fliegl, A. Köhn, C. Hättig and R. Ahlrichs, *J. Am. Chem. Soc.*, 2003, **125**, 9825.

[62] M. Eisenberg and D. D. Des Marteau, *Inorg. Chem.*, 1972, **11**, 1901.

[63] D. D. Des Marteau, *J. Am. Chem. Soc.*, 1969, **91**, 6211.

[64] T. L. Charlton and R. G. Cavell, *Inorg. Chem.*, 1969, **8**, 2436.

[65] V. A. Sipachev, *J. Mol. Struct.*, 1985, **121**, 143.

[66] A. J. Downs, G. P. Gaskill and S. B. Saville, *Inorg. Chem.*, 1982, **21**, 3385.